

RECLAMATION

Managing Water in the West

**Hydraulic Laboratory Technical Memorandum
No. TER-CAS-8460-2013-1**

Terminal Dam Corrective Action Study – Jet Erosion Tests of Embankment Soils and WinDAM B Breach Modeling



**U.S. Department of the Interior
Bureau of Reclamation
Technical Service Center
Hydraulic Investigations and Laboratory Services Group
Denver, Colorado**

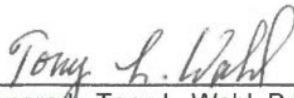
September 2013

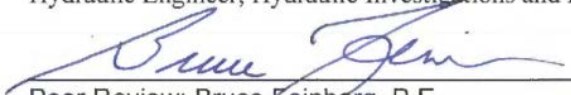
BUREAU OF RECLAMATION
Technical Service Center, Denver, Colorado
Hydraulic Investigations and Laboratory Services, 86-68460

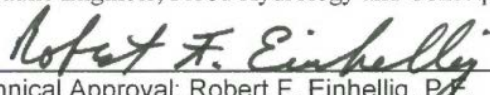
Technical Memorandum No. TER-CAS-8460-2013-1

**Terminal Dam Corrective Action Study –
 Jet Erosion Tests of Embankment Soils
 and WinDAM B Breach Modeling**

Solano Project, California
Mid-Pacific Region

 9/19/13
 Prepared: Tony L. Wahl, P.E.
 Hydraulic Engineer, Hydraulic Investigations and Laboratory Services, 86-68460

 9/19/13
 Peer Review: Bruce Feinberg, P.E.
 Hydraulic Engineer, Flood Hydrology and Consequences Group, 86-68250

 9/25/13
 Technical Approval: Robert F. Einhellig, P.E. Date
 Manager, Hydraulic Investigations and Laboratory Services, 86-68460

REVISIONS					
Date	Description	Prepared	Checked	Technical Approval	Peer Review

Introduction

Terminal Dam, completed in 1959, is a small (approximately 100 acre-ft) off-stream reservoir located about 7 miles southwest of Fairfield in central California at the terminus of the Putah South Canal. The reservoir is formed by two small homogeneous compacted embankments, the Northeast Auxiliary Dam and the South Dam, both about 24 feet high. The reservoir is filled through the Green Valley Siphon, which enters the reservoir through the Northeast Auxiliary Dam. Water is released from the reservoir through the outlet works that pass through the South Dam near its right abutment.

Terminal Dam is located in a seismically active area, and residential development in recent years downstream from both embankments (see Figure 1) makes it necessary to evaluate the risks associated with a potential dam breach. This technical memorandum documents field investigations of the erodibility of the embankment soils and numerical modeling of potential dam breach scenarios associated with seismically triggered failure modes. The objective of the modeling work was to estimate the dam breach outflow hydrograph at the dam site itself; modeling of flood propagation and downstream inundation potential will be performed separately.



Figure 1. — Terminal Reservoir location map.

Project History

The design, construction and operating history for Terminal Dam is summarized below from more detailed information assembled by Schenk McFarland (2010) [9].

Design and Construction

The facility commonly known as Terminal Dam and Reservoir includes the South Dam, the Northeast Auxiliary Dam (NE Auxiliary Dam), and an outlet works built between 1958 and 1959. Historically, the South Dam has at times been referred to as the “Main Dam” or “Terminal Dam”, but for simplicity this report uses “South Dam” to indicate the south embankment specifically, and “Terminal Dam” to collectively indicate the dual embankments that impound Terminal Reservoir. The facility is a feature of the Solano Project, a multipurpose development supplying water for agricultural, municipal, and industrial purposes in Solano County, CA.

The two embankments are homogeneous, constructed of clay soils with plasticity index (PI) values ranging from about 16 to 32, mostly around 20. Both dams are 24 ft high, with design crest elevations of 93.5 ft and design crest widths of 20 feet. Upstream embankment slopes are 3H:1V, covered with coarse gravel and cobbles. Downstream embankment slopes are 2H:1V, with sparse grass cover. The South Dam is 500 ft long, and the NE Auxiliary Dam is 870 ft long. Currently, the crest width of the South Dam is somewhat wider than 20 ft due to additional material placed on the upstream slope after construction. The reservoir has a design storage capacity of approximately 119 ac-ft at design maximum water surface elevation 89.67 ft, although deposition in the reservoir has reduced its capacity to about 100 ac-ft at this time. All modeling for this study was based on an undated area-capacity curve shown in Figure 2.

The reservoir is filled by flow from the Putah South Canal conveyed through the Green Valley Siphon. The only release facility at the dam is the reservoir outlet works located in the embankment of the South Dam near the right abutment. The outlet works consists of a 69-inch-diameter concrete pipe at invert elevation 77.56 ft, a tower housing two 42-inch-diameter cast-iron slide gates with manual operators, and a bifurcation to two 42-inch-diameter concrete pipes. These pipes feed the City of Vallejo pump house and City of Benecia pump house. There is an overflow structure (wasteway) located about 1 mile from the dam at the Putah South Canal/Green Valley Siphon Structure on the east side of Green Valley. When the elevation head and pressure head exceed 89.5 feet, supply water passes the overflow structure and flows through the wasteway pipe to Green Valley Creek. When the reservoir water surface is higher than the canal water surface, the flow reverses through the siphon and spills down the wasteway pipe into Green Valley Creek. Since this is a gravity system, the elevation of the wasteway limits the maximum reservoir water surface elevation. The reservoir can be evacuated through the Green Valley Siphon to the elevation of the invert of the siphon and through the outlet works located in the embankment of the South Dam.

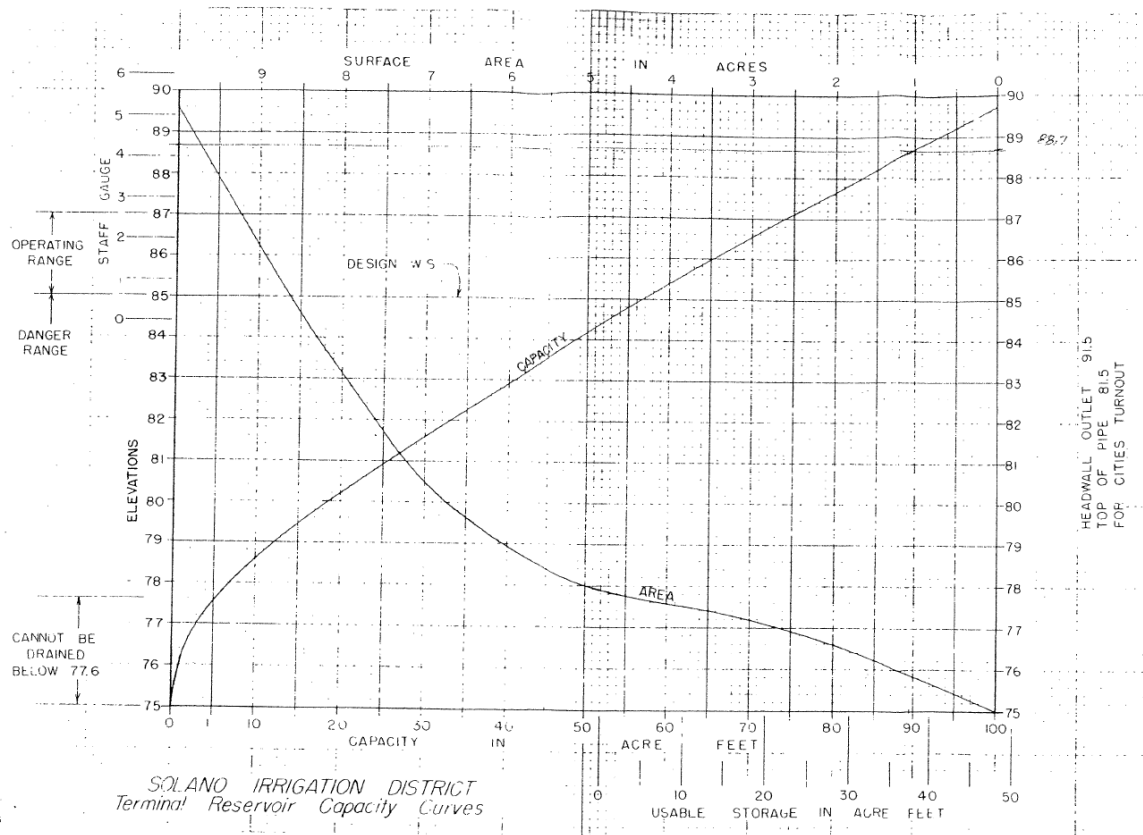


Figure 2. — Area-capacity curve for Terminal Dam and Reservoir.

Design and construction information for these structures is extremely limited. The specification under which the embankments were constructed primarily addresses the Putah South Canal and the Green Valley Siphon. Only one design drawing for the two embankments has been located (Figure 3). Both embankments were constructed as homogeneous dams utilizing locally available material, primarily obtained from the reservoir area. Typical construction practice in the 1950's included placement in lifts and specified compaction procedures, but the details are unknown. It is likely that the embankments used select borrow materials, and this appears to be confirmed in the limited data available. Two drill holes completed in 2004 provided several samples of the embankment materials; they showed that both embankments are generally composed of sandy clay and clayey sand with little to no gravel. The design drawing shows that the borrow area for the embankment materials was located in the northwest corner of the reservoir. The geology of this area suggests this is landslide debris, but that is uncertain. Available drill hole logs (1956) from the reservoir borrow area indicate mostly lean clays and some fat clays although sands and silts are also noted. Table 1 summarizes soil test information for each embankment.

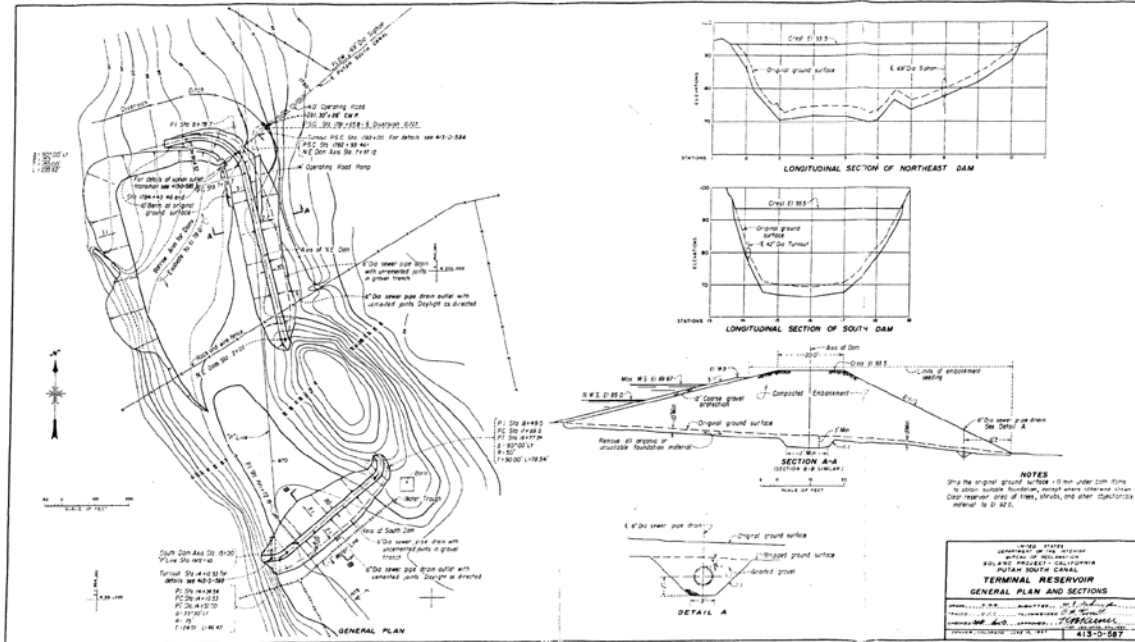


Figure 3. — Terminal Reservoir embankment design drawing, 413-D-587.

Table 1. — Embankment soil properties (see [9] and [10]).

Data source	Parameter	South Dam	NE Auxiliary Dam
Drill logs, 2004 embankment drill holes	Soil types	sandy fat clay with minor gravel (CHg), clayey sand/sandy fat clay with minor gravel (SC/CH), and sandy fat clay (sCH)	clayey sands with minor gravel (SCg), fat clay with sand (CHs), sandy fat clay (sCH), and clayey sand/sandy fat clay (SC/CH)
	Gradation	50 to 60% fines	60 to 80% fines
	Hand tests	“medium to high” toughness; “high” dry strength	medium toughness; dry strength ranging from “low to medium” to “high.”
Laboratory tests of embankment samples	Soil types	sandy lean clay, lean clay with sand, and fat clay with sand	sandy lean clay with gravel, clayey gravel with sand, sandy lean clay, sandy fat clay and fat clay with sand
	Gradation	38 to 85% fines; 37% < 0.005 mm (median of 9 samples); approx. 15 to 60% sand; max 1.9% gravel;	47 to 75% fines; 32% < 0.005 mm (median of 7 samples); 20 to 36% sand; 0 to 31% gravel
	Plasticity Index (PI)	21 to 32	16 to 32
Strength testing			
Torvane shear tests (field)	undrained shear strength, c_u	1,840 to 4,100 lb/ft²	1,150 to 3,070 lb/ft²
Pocket penetrometer (lab)	unconfined compressive strength, q_u	2,563 to 7,170 lb/ft ²	4,090 to 7,170 lb/ft ²
	undrained shear strength ($c_u=q_u/2$)	1,280 to 3,590 lb/ft²	2,045 to 3,590 lb/ft²

Strength testing of embankment samples from the South Dam was performed in the laboratory and in the field in association with the 2004 drilling operations. There is conflict between laboratory and field reports of Torvane shear test results (undrained shear strength). The laboratory numbers seem extraordinarily high and are suspected of being misreported [9]. (It seems likely that they were measured in kPa but erroneously reported with units of lb/in².) The lower (and likely more reasonable) values come from the field tests, reported in the Draft Interim Summary Report, Terminal Dam Drilling and Hole Completion [8]. Pocket penetrometer tests performed in the laboratory [10] are consistent with this interpretation. The strength data will be relevant as input to the WinDAM B dam breach model discussed later in this report.

The field and laboratory soil classification information and strength tests all indicate a material that should make a good, strong clay core for a zoned embankment, and has appeared to be sufficient for the homogeneous embankments that were constructed. The soils in the NE Auxiliary Dam contain more gravel than those of the South Dam, but the differences are minor from a performance standpoint, and in general the two embankments have very similar physical properties. Although it is clear that the embankment materials were compacted, no information is available on the specific compaction procedures used. Moisture content, lift thickness, number of passes, etc. cannot be confirmed. Based on a review of available gradation data, the material is expected to have low permeability and fairly high shear strength.

Sinkhole and Conduits through Embankments

The soils used to construct Terminal Dam are generally regarded as erosion and earthquake resistant. However, in March 2002 a sink hole was discovered near the crest of the South Dam above the downstream 42-inch-diameter precast concrete outlet works pipe. The sink hole was excavated and loose material was followed to a pipe used for municipal water supply. Gaps ¼ to ½ inch wide were discovered at the joints between internal compression bands in the City of Vallejo concrete pipe. Other than the joint connections, the pipe was in generally good condition. It was determined that the sink hole was likely caused by embankment material being sucked into open joints in the pipe as pumps were operating. Pipe repairs were reportedly completed in 2003 or 2004 by sealing the joints. The outlet works pipe has reportedly operated satisfactorily since that time. Only the City of Vallejo pipe was inspected; the City of Benicia pipe that was originally constructed using the same techniques has not been dewatered and inspected.

The outlet works and siphon conduits do not meet current Reclamation design standards. Both conduits were constructed from precast concrete pipe laid directly on the foundation, with unreinforced joints and large seepage collars. In a typical, modern dam design, conduits passing through an embankment would be reinforced, cast-in-place horseshoe shapes to facilitate compaction around the conduit and provide a stout conduit that would resist potential movements of the embankment. Seepage collars would not be included, as they hinder proper compaction of soil around the conduit and are considered detrimental.

Seismic Hazard

The seismic hazard at this site is among the highest in Reclamation's dam inventory. The probabilistic seismic hazard study completed for the Comprehensive Facility Review (CFR) indicates an earthquake with a return period of 500 years is capable of producing a mean peak horizontal acceleration (PHA) of 0.96g and that an earthquake with a return period of 1,000 years is capable of producing a PHA of 1.2g. In addition, Strands 3 and 4 of the Green Valley Fault system likely cross beneath the embankments. This is considered to be an active fault system, with an estimated 1 in 500-yr displacement of about 1 m and 1 in 2,000-yr displacement of roughly 2 m.

Several residential subdivisions and other dwellings have been constructed immediately downstream from the embankments since Terminal Dam was constructed. If a dam breach were to occur, breach outflows would travel through residential subdivisions across Reservoir Lane.

Jet Erosion Testing

Submerged jet erosion tests were conducted at the dam site on March 4-5, 2013 to determine erodibility parameters for the embankments and support computer modeling of potential dam breaches. The tests were performed using a test apparatus constructed by Reclamation in accordance with ASTM D-5852, *Standard Test Method for Erodibility Determination of Soil in the Field or in the Laboratory by the Jet Index Method* [1]. This test uses measurements of the scour caused by an impinging hydraulic jet to quantify the erodibility of fine-grained soil materials. A schematic diagram of the test setup is shown in Figure 4. Head is provided to the jet tube from an adjustable head tank that can be raised up to 20 ft above the test specimen. The shear stress applied to the sample by the jet can be regulated by adjusting the jet pressure and the initial distance between the nozzle and the soil surface. A detailed description of Reclamation's laboratory and field jet test facilities is available in Wahl et al. (2008).

Measurements of scour depth versus elapsed time are analyzed by a curve-fitting procedure described in Hanson and Cook (2004) to determine two parameters of an erosion equation based on the excess stress concept:

$$\dot{\varepsilon} = k_d (\tau - \tau_c)$$

where $\dot{\varepsilon}$ is the volume of material removed per unit surface area per unit time ($\text{m}^3/\text{s}/\text{m}^2$, or m/s), k_d is a detachment rate coefficient, τ is the applied shear stress, and τ_c is the critical shear stress needed to initiate erosion. The test produces estimates for the values of k_d and τ_c . Typical S.I. units for k_d are $\text{m}^3/\text{s}/\text{m}^2/\text{Pa}$, which reduces to $\text{m}/\text{s}/\text{Pa}$ or $\text{m}^3/(\text{N}\cdot\text{s})$; k_d is also commonly reported in $\text{cm}^3/(\text{N}\cdot\text{s})$. When working in U.S. customary units, k_d is usually expressed in $\text{ft}/\text{hr}/\text{psf}$ [$1 \text{ cm}^3/(\text{N}\cdot\text{s}) = 0.5655 \text{ ft}/\text{hr}/\text{psf} = 10^{-6} \text{ m}^3/(\text{N}\cdot\text{s})$]. Typical units for τ_c are Pa or lb/ft^2 (psf).

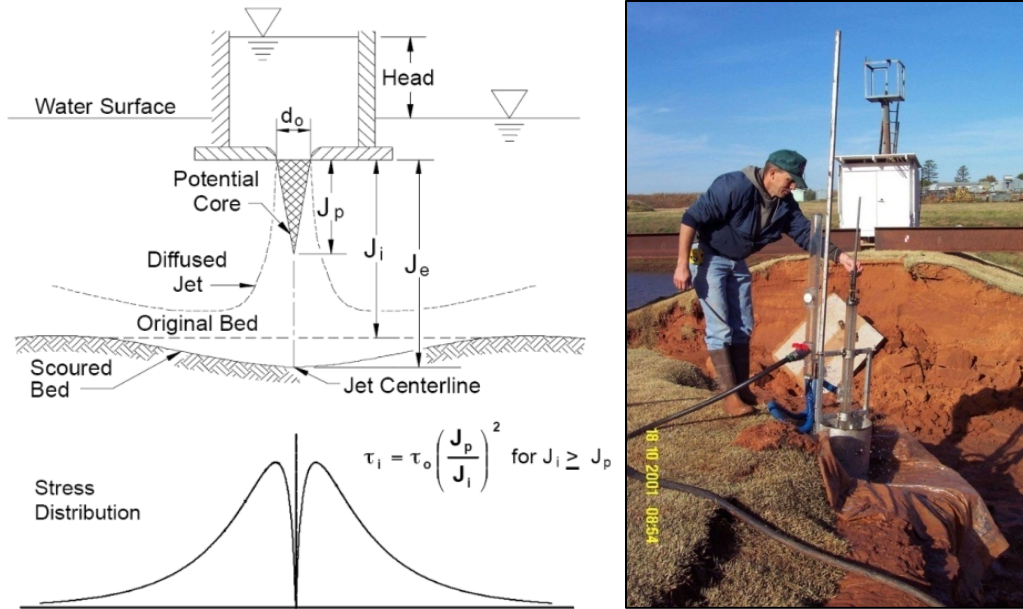


Figure 4. — Schematic of circular submerged jet erosion test (from Hanson and Cook 2004), and photograph of a field test in progress following an experimental embankment breach event (USDA-ARS, Hydraulic Engineering Research Unit, Stillwater, Oklahoma).

Jet erosion tests can be performed in the field or in the laboratory using undisturbed samples (tube samples) or remolded samples (e.g., compaction test specimens). The advantage of *in situ* testing in the field is that the soil can be tested in its existing compaction state with minimal risk of disturbance during sampling and transport to the laboratory. Since water chemistry can affect erodibility, it is also advantageous to conduct tests with a water source representative of the water that might eventually erode the material during a real event.

To evaluate the erodibility of the two embankments, a total of six jet tests were performed, one each over the Green Valley Siphon and outlet works conduits, and two near the maximum section of each embankment, one high on the embankment and the other at a lower position. All tests except the one over the outlet works conduit were performed on the downstream slopes of the embankment, since erosion and headcutting into the downstream slope is crucial during the initiation of a breach, and because access to the upstream slope was limited by the reservoir water level and the riprap layer covering the upstream slope. The test over the outlet works conduit was performed on the upstream side because access roads limited exposure of representative embankment materials over the conduit. The tests over the inlet and outlet conduits represented locations with the greatest potential for a seismic-induced failure, and the tests at the maximum sections represented locations with the greatest potential for a deep breach and large peak breach outflow.

Test sites were established by hand excavation to create a near-horizontal shelf large enough to accommodate the 1-ft diameter submergence tank. The head tank was situated uphill from the test site, and the initial distance from the nozzle to the ground surface was adjusted to put the initial jet stress into a range similar to the shear stresses that might be

experienced during a dam breach event (estimated to be 1.3 to 1.9 lb/ft²). Water was then pumped from the reservoir over the dam to the head tank during the test. At regularly increasing time intervals (typically 1 min, 2 min, 4 min, 8 min, 16 min, etc.), the depth of scour produced by the jet was recorded. Most tests lasted about 30 to 90 minutes, depending on the rate of observed erosion. As each test progressed, deepening of the scour hole beneath the jet caused the applied stress to be reduced and the erosion rate to generally diminish. Figure 5 shows a typical setup of the jet test equipment.



Figure 5. — Jet test in progress on NE Auxiliary Dam, site number 3, and a post-test photo of the scour hole produced during test number 6.

Despite care exercised during hand excavation to prepare each test site, there was some disturbance of the soil, especially in the uppermost layers. Thus, in many of the tests, very rapid erosion was observed during the first 1 min time interval as disturbed material was removed. In these tests (1, 4, 5, and 6), the data were analyzed by discarding the first data point, essentially considering the tests to effectively begin after 1 minute of time had elapsed. This initial rapid erosion was not observed in tests 2 and 3 and all data collected during those test was utilized.

Table 2 summarizes the test results, and Figure 6 shows the erodibility parameters plotted with respect to erodibility classifications suggested by Hanson and Simon (2001) from a study of cohesive natural streambeds. The crucial parameter related to erosion of the embankments during a breach event is the detachment rate coefficient, k_d , which affects the rate of headcut advance and breach enlargement. The critical shear stress values are relatively low compared to stresses that will occur during a dam breach, so the value of τ_c is inconsequential and is often assumed to be zero during dam breach modeling.

Table 2. — Summary of jet test results.

Test No.	Location	Longitude	Latitude	Initial stress, τ_0	Final stress, τ_f	τ_c	k_d
				psf	psf	psf	ft/hr/psf
1	South Dam, d/s slope, 5-ft below crest	122°09.524' W	38°13.144' N	0.31	0.132	0.0193	1.14
2	Over outlet pipe, u/s slope	122°09.567' W	38°13.123' N	1.58	0.538	0.0137	2.45
3	NE Dam, mid section, 6-ft below crest, d/s slope	122°09.564' W	38°13.276' N	2.11	1.039	0.136	0.116
4	Above inlet pipe at NE corner of reservoir, about 5' below crest, downstream slope	122°09.589' W	38°13.329' N	0.35	0.168	0.0421	1.38
5	NE Dam, low on downstream slope	122°09.564' W	38°13.280' N	0.34	0.201	0.0544	0.886
6	South Dam, low on downstream slope	122°09.524' W	38°13.143' N	0.58	0.094	0.00104	2.27

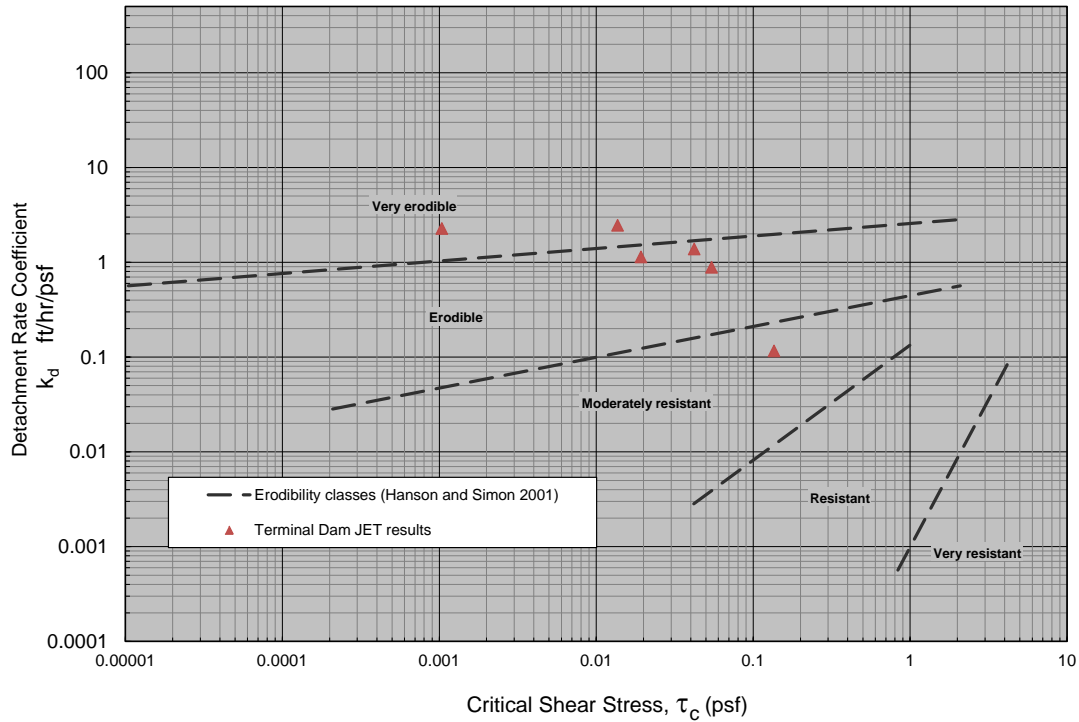


Figure 6. — Erodibility test results compared to descriptive classifications established by Hanson and Simon (2001) for cohesive stream channel deposits.

The two tests with the highest values of k_d plot in the very erodible range of Figure 6. However, these values (approximately 2.0 to 2.5 ft/hr/psf) are still much lower than values seen in poorly compacted embankments or in soils with little to no plasticity, which can range as high as 400 ft/hr/psf (Hanson et al. 2010).

Table 3. — Approximate values of k_d in $\text{cm}^3/(\text{N}\cdot\text{s})$ as a function of compaction conditions and %clay (Hanson et al. 2010). [$1 \text{ cm}^3/(\text{N}\cdot\text{s}) = 0.5655 \text{ ft/hr/psf}$]. Shaded cells indicate range of possible conditions for Terminal Dam embankments.

% Clay (<0.002 mm)	Modified Compaction (56,250 ft-lb/ft ³)		Standard Compaction (12,375 ft-lb/ft ³)		Low Compaction (2,475 ft-lb/ft ³)	
	≥Opt WC%	<Opt WC%	≥Opt WC%	<Opt WC%	≥Opt WC%	<Opt WC%
Erodibility, k_d , $\text{cm}^3/(\text{N}\cdot\text{s})$						
>25	0.05	0.5	0.1	1	0.2	2
14-25	0.5	5	1	10	2	20
8-13	5	50	10	100	20	200
0-7	50	200	100	400	200	800

For comparison, Hanson et al. (2010) provided guidance for estimating values of k_d in situations where jet testing is not practical or feasible. Table 3 shows the suggested values of k_d depending on clay content, compaction energy, and water content at time of compaction. To use the table we need estimates of the compaction energy, water content at time of compaction, and clay content. USDA and USBR use different definitions for the clay-size fraction (USDA < 0.002 mm; USBR < 0.005 mm); the laboratory tests from the 2004 embankment drill hole samples [10] showed median values of clay content by the USBR definition to be 37% in the South Dam and 32% in the NE Auxiliary Dam (see Table 1), and gradation analyses were not carried below 0.005 mm for most samples. Thus, the specific data we need are not fully available, but it is likely that the % finer than 0.002 mm is at least 14% and perhaps greater than 25%. We do not know the compaction conditions that apply to Terminal Dam, but if we assume standard compaction effort and consider the possibility of dry, optimum, or wet compaction, then k_d values of 0.1 to 10 cm³/(N-s) are possible (0.057 to 5.7 ft/hr/psf). The measured values of k_d shown in Table 2 (0.116 to 2.45 ft/hr/psf) are in the middle of this range. Thus, the field test results appear to be reasonable.

Dam Breach Modeling

To facilitate analyses of potential downstream flooding during a dam breach event, the WinDAM B model (Version 1.1; August 2012) was applied to the Terminal Dam embankments to simulate the potential time-history of erosion, breach development, and breach outflow. The simulations considered only seismic-induced failure modes, in which the development of a transverse crack in an embankment allows erosion to occur that leads to uncontrolled release of the reservoir. Breach hydrographs produced by static failure modes (sunny-day failures by internal erosion) are expected to be substantially similar, although details of the breach initiation process and timing may vary.

The WinDAM B model was developed by the U.S. Department of Agriculture for simulating potential dam breaches of homogeneous embankment dams. The triggering event for a WinDAM B simulation is overtopping of the embankment. A version of WinDAM (“C”) that will support internal erosion-caused failures is still under development. WinDAM B is distributed by the Natural Resources Conservation Service. The erosion modeling technology was primarily developed by the Agricultural Research Service at their Hydraulic Engineering Research Unit in Stillwater, Oklahoma. Although initially released in late 2011, comprehensive documentation for the model is not yet available. Primary references for the model and its underlying technology are listed in an appendix at the end of this report.

The potential failure mode of concern for these simulations was erosional breach by flow through a transverse crack in the embankment caused by a seismic event. Although not a classical overtopping flow situation, the WinDAM B model could be applied reasonably to this failure mode, since the model allows the user to define a non-uniform crest profile for the embankment along its length. The intent of offering this capability in WinDAM B

is to allow a simulation to consider the effects of flow concentration due to camber or settlement of the embankment, but it also allows the definition of a pilot channel through the embankment that can simulate the spontaneous development of a transverse crack that extends below the reservoir water level. Flow through this crack can take place in the model and is able to drive a headcut development and advancement process that will breach the dam.

Simulations were performed assuming that a breach took place at the maximum section of the South Dam, which has a dam base elevation of 70 ft (original ground surface). This location was selected because it can produce the deepest breach and largest peak outflow, and because it is possible for a crack to develop here (but perhaps is more likely in other locations). The NE Auxiliary Dam has a similar maximum section, with the original ground surface elevation at the base of the dam equal to about 72 ft. Simulations specific to this dam base elevation were not performed; the effect would likely be only a slight reduction in peak breach outflow. For all simulations the dam crest width at elevation 93.5 ft was set to 20 ft, upstream embankment slope was 3H:1V, and downstream embankment slope was 2H:1V. The original design area-capacity curve was utilized, and the simulations were carried out with a low tailwater curve defined for the downstream channel, so that there would be no restriction of the breach outflow due to tailwater effects. The starting reservoir elevation for all simulations was set to 89.67 ft, the design maximum water surface. For all model runs the total unit weight of the embankment soil was estimated to be 124 lb/ft³.

An important modeling decision in WinDAM B is the selection of the headcut model. WinDAM B allows the use of either the Hanson/Robinson stress-based model or the Temple/Hanson energy-based model. The stress-based model is a physically-based approach that typically is the best choice for dams that are tall or composed of relatively weak soils. The energy-based model is an empirically-based method, primarily calibrated against data from laboratory breach tests of embankments in a 5 to 20-ft height range. Since the Terminal Dam embankments are only 24 ft high and contain soils with moderate to high clay content and plasticity indices of 16 to 32, a strong argument could be made for using the energy-based model. However, there is no clear-cut guidance for selecting the headcut model, and testing showed that the stress-based model produced faster breaches with larger peak outflows (about twice as large) for this application. To ensure a conservative result, the stress-based model was used to generate all model results reported in this document.

Three key parameters define the erodibility of the embankment soil in the WinDAM B model: the detachment rate coefficient (k_d); the critical shear stress (τ_c); and the undrained shear strength (c_u). The first two parameters were estimated using the submerged jet erosion test results, and the undrained shear strength was set on the basis of the soil strength measurements obtained from the 2004 embankment drill hole samples, and using guidance provided by the WinDAM B developers, shown in Table 4. For each parameter, a range of reasonable values was established, as shown in Table 5.

Table 4. — Estimating undrained shear strength for use in WinDAM B (Hanson et al. 2011).

Consistency	Description	Undrained shear strength, c_u (psf)
Very soft	Exudes between fingers when squeezed in hand	< 420
Soft	Easily molded with fingers, point of geologic pick easily pushed into shaft of handle	420 – 840
Firm	Penetrated several cm by thumb with moderate pressure. Molded by fingers with some pressure.	840 – 1570
Stiff	Indented by thumb with great effort. Point of geologic pick can be pushed in up to 1 cm. Very difficult to mold with fingers. Just penetrated with hand spade.	1570 – 3140
Very stiff	Indented only by thumbnail. Slight indentation by pushing point of geologic pick. Requires hand pick for excavation.	3140 – 6540

Table 5. — Estimated WinDAM B soil erodibility parameters for Terminal Dam embankments.

Parameter	More erodible estimate	Best estimate	Less erodible estimate
Detachment rate coefficient, k_d	2.5 ft/hr/psf (upper end of measured values from jet tests)	1 ft/hr/psf (approx. median/mode of measured values)	0.5 ft/hr/psf (average of two lowest measured values)
Critical shear stress to initiate erosion, τ_c	0 psf	0.01 psf	0.05 psf
Undrained shear strength	1200 psf (low end of measured values; middle of “firm” consistency class)	1600 psf (middle of measured values; boundary of “firm” and “stiff”)	2400 psf (approx. upper end of measured values; middle of “stiff” range)

An initial set of simulations was used to explore sensitivity to the parameters that define the initial transverse crack in the dam. These simulations were all performed using the “more erodible” values shown in Table 5. Key parameters that define the configuration of the initial crack in the dam are its width and depth. Testing showed that the breach initiation and development were insensitive to the initial crack width, but very sensitive to the initial crack depth. The reasons for this behavior became apparent after studying the details and intermediate conditions of several runs. Figure 7 shows a sequence of charts illustrating the elevation profile (top) and plan view of the headcut and widening breach channel (bottom) during one run of the model. Figure 8 shows a cross-section of the embankment that illustrates terminology and parameters of interest in the discussion that follows.

Key observations made from the initial series of test runs were:

- Flow through the initial crack is simulated in WinDAM B as a broad-crested weir flow. The total discharge is related to the crack width and the depth of the crack (i.e., reservoir head above the crack invert). The unit discharge through the crack is related only to the depth of the crack. (The broad-crested weir assumption is not strictly accurate for a very narrow crack, which would probably experience some degree of orifice-type flow control and/or significant frictional resistance from the sides of the crack, but unit discharge would still be primarily a function of the crack depth and relatively independent of crack width.)

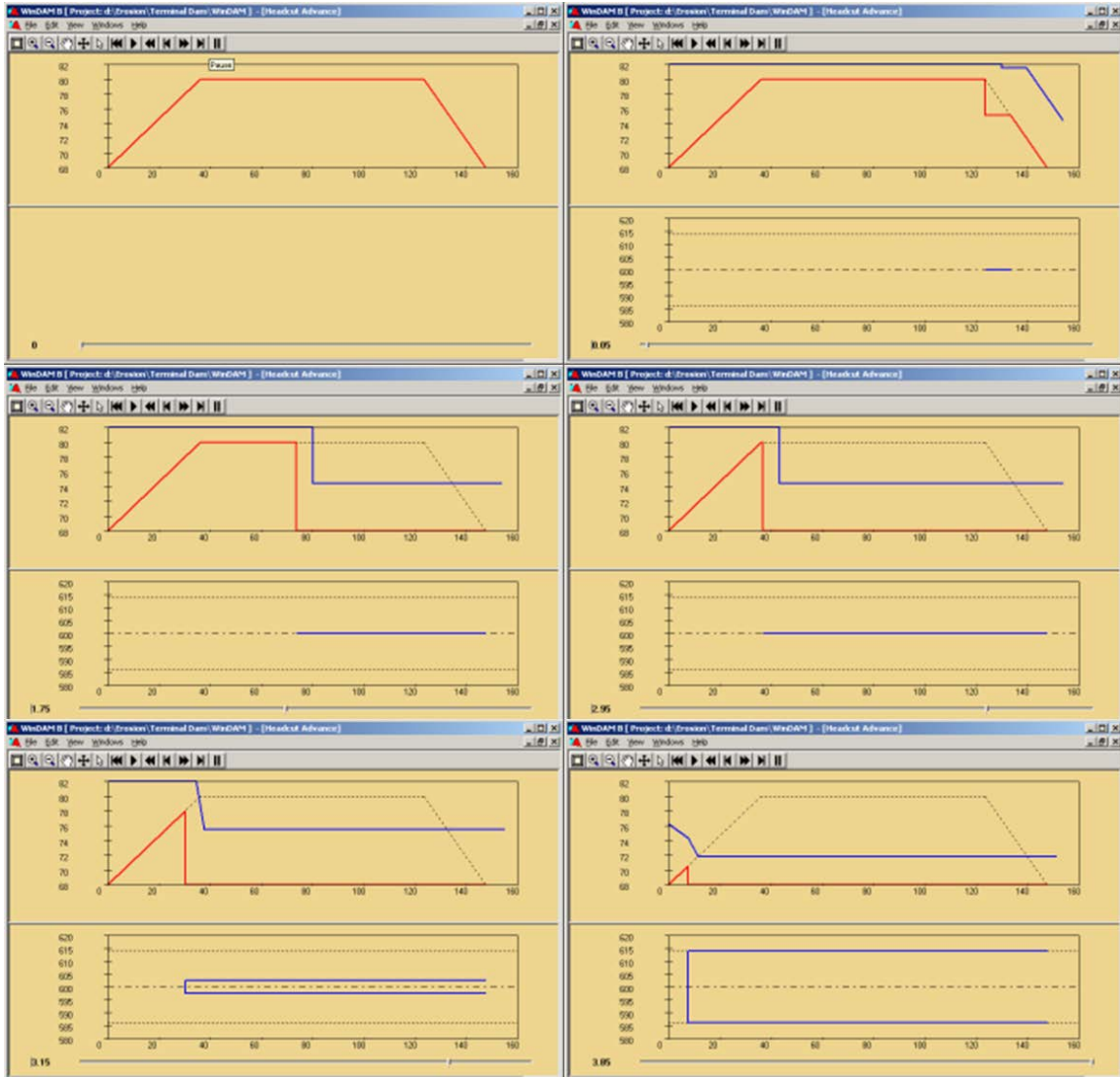


Figure 7. — Sequence of charts showing evolution of a breach channel starting from an initial deep, narrow transverse crack in the embankment. The red line indicates the embankment outline and the invert of the transverse crack as the headcut develops and advances. Elapsed time in hours is indicated in the lower left corner of each chart.

- The flow through the crack causes incision of a gully into the downstream face of the dam, below the point where the crack exits onto the downstream slope. This creates a headcut that deepens until its height is equal to the difference between the initial crack bottom elevation and the base of the dam. The headcut advances upstream toward the reservoir, and the crack does not widen in the WinDAM B model until the headcut reaches the reservoir. In reality, the crack probably will widen somewhat during this time, but the primary erosion will be taking place at the base of the outfall from the crack (the headcut), which is what is modeled by WinDAM B. The process of headcut advance prior to the headcut reaching the reservoir is referred to as *breach initiation*.

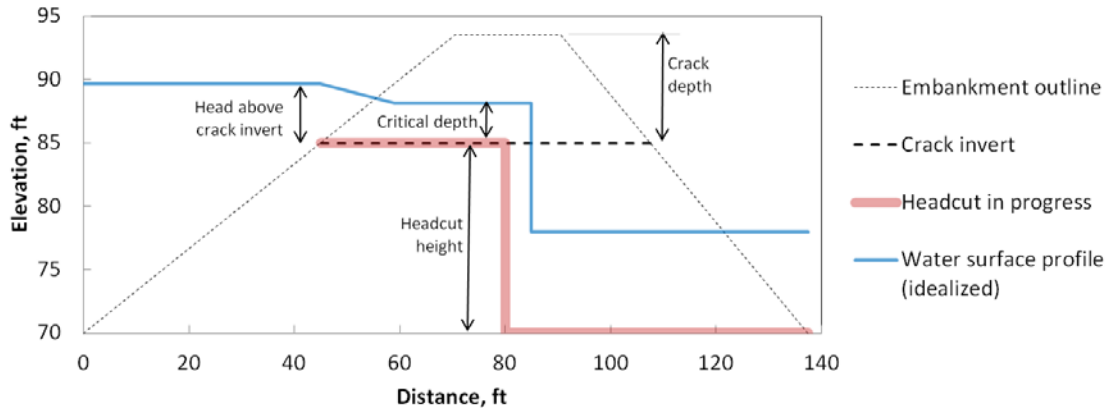


Figure 8. — Cross-section view of embankment during headcut advance phase, illustrating terminology and important physical parameters for the WinDAM B model.

- The rate of headcut advance increases with both the unit discharge through the crack and the height of the headcut. A wider initial crack does not change the unit discharge, so it does not change the rate of headcut advance. A deeper crack increases the unit discharge, but also reduces the height of the headcut. Thus, starting with a shallow crack, the net effect is that the headcut advance rate will first increase with increasing crack depth, reach a maximum, then decrease again when the headcut height becomes low. There is an optimal crack depth that causes a maximum rate of headcut advance. Tests performed later in the investigation attempt to quantify this.
- A key concept in the model is that headcut advance can only occur when the headcut height is greater than the critical depth of flow at the brink upstream from the headcut. With a very deep initial crack, the headcut height will be less than the depth of critical flow through the crack (recall that flow through the crack is modeled as weir flow), so the model does not allow the headcut to advance, nor does the crack widen. In some cases, this condition will exist at the outset of a run, so there is no initial headcut advance, but headcut advance will occur after the reservoir has dropped enough to reduce the critical depth to less than the headcut height. This behavior is somewhat counterintuitive and may not be realistic of how a deep crack would behave. However, this situation only occurs for cracks that are deeper than what is considered reasonable for this application, and only for crack depths that are lower than those at which the peak breach outflow begins to diminish for some of the other reasons discussed above.
- Widening of the crack begins when the headcut breaches into the reservoir. This phase of the process is often called *breach enlargement*, *breach formation*, or *breach development*. Total discharge increases dramatically from this point onward, until the reservoir is drained sufficiently to again reduce the flow rate. A deeper crack widens more rapidly and produces a larger peak outflow due to greater reservoir head above the crack invert and larger unit discharge through the crack.

- A wider crack does not increase the rate of headcut advance or the rate of breach widening, but it does drain the reservoir more rapidly during the breach initiation phase. This causes the reservoir head to be reduced when breach enlargement begins, so a wider initial crack tends to produce a lower peak outflow, which is a counterintuitive result. Appendix C shows results of several simulations performed to demonstrate this behavior.

These observations led to the conclusion that a fixed crack width could be used, and a value of ½ inch was considered to be a reasonable estimate by those familiar with the embankments and the seismic events of concern (Tonya Hart and Tara Schenk McFarland, 86-68313). It was also determined that a range of crack depths should be explored in order to find the crack depths that would lead to the most rapid headcut advance and high peak outflows. Thus, for each combination of soil erodibility parameters (“more erodible”, “less erodible”, and “best estimate”), multiple model runs were made with a range of crack depths. For each crack depth, the dam crest width defined in the model was adjusted to reflect the length of the transverse crack through the dam at the invert, not the 20-ft width of the top of the dam at elev. 93.5 ft. This causes the model to simulate the correct distance of headcut advance needed to produce a breach into the reservoir. The changing crack length is another factor tending to cause very deep cracks to exhibit slower breach initiation and associated smaller peak outflows.

Figure 9 shows the results of the multiple dam breach simulations across different crack depths and the three different sets of soil erodibility parameters. The crack depth needed to produce maximum peak outflow ranges from 13.5 to 15.75 ft, depending on the soil erodibility parameters. Peak outflow ranges from 1,960 to 605 ft³/s, with the best-estimate case producing a peak outflow of 1,120 ft³/s. Based on geotechnical considerations, crack depths of 10 to 20 ft were believed to be reasonable for the anticipated seismic event scenarios being considered.

For the case of the more erodible soil parameters, the breach initiation time is 3 to 6 hours, depending on initial crack depth, and the breach formation time (elapsed time between first advance of the headcut into the reservoir and the time of peak outflow) is about 0.35 hr (21 min) in the most severe case. The initiation time translates into potential time for warning and evacuating downstream areas following a seismic event that cracks the embankment. The breach formation time is significant for modeling the evolution of the breach opening that regulates reservoir outflow. For the best-estimate case, the breach initiation time is 8 hours or more, depending on crack depth, and the breach formation time is about 0.7 hr (42 min). For the less erodible set of soil parameters, breach initiation requires 18 hr or more and breach formation time is about 1.2 hr (72 min). During the breach initiation phase, WinDAM B predicts very low flow rates and essentially no increase in the outflow rate until the breach formation phase begins. In reality there is probably a slow rate of outflow increase during breach initiation due to some widening of the initial crack, but flow rates should be non-lethal during this period.

Figure 10 shows variation of the predicted breach width for different initial crack depths and each set of soil erodibility parameters. About one-half to two-thirds of the breach widening occurs prior to the occurrence of the peak outflow. At the crack depths that produce the maximum peak outflows, predicted breach width at peak outflow varies from about 7 to 20 ft, depending on soil erodibility, and final breach width varies from about 11 to 30 ft.

Figure 11 shows the time history of breach outflow and breach width for one specific simulation, the case of best estimate soil parameters and an initial crack depth of 13.5 ft. This case produces a peak outflow of 797 ft³/s.

Comparison to Traditional Dam Breach Analysis

A traditional approach to dam breach analysis has been the use of regression equations to predict breach width and breach formation time, followed by dam-break flood simulation using a computer model such as HEC-RAS. Alternately, regression equations can be used to estimate peak breach outflow directly. A comparison of WinDAM B results to these more traditional approaches was made.

Wahl (2004) evaluated numerous breach parameter prediction equations to determine their mean prediction errors and uncertainties when applied to a database of real dam failure case studies. Some preferred methods identified in this study were:

- Breach width – Von Thun & Gillette (1990); Froehlich (1995a);
- Breach formation time – Von Thun & Gillette (1990); Froehlich (1995a);
- Peak breach outflow – Froehlich (1995b); Walder & O'Connor (1997);

In addition to the methods studied in Wahl (2004), new work by Froehlich (2008) provides updated equations for breach width and breach formation time.

It is notable that there are no established methods for predicting breach initiation time; this is because in the early history of dam breach modeling, the purpose for estimating breach formation time was traditionally to allow accurate modeling of the increase of breach size and the resulting outflow. Only in more recent years did the importance of breach initiation and warning time for predicting loss of life become apparent, but methods for making quantitative predictions of breach initiation time have never been well developed. There is little doubt that the breach formation time data for historic failures do include some of the breach initiation phase, since it is very difficult in practice to clearly delineate between the two phases, especially for lay persons who often witness dam breach events.

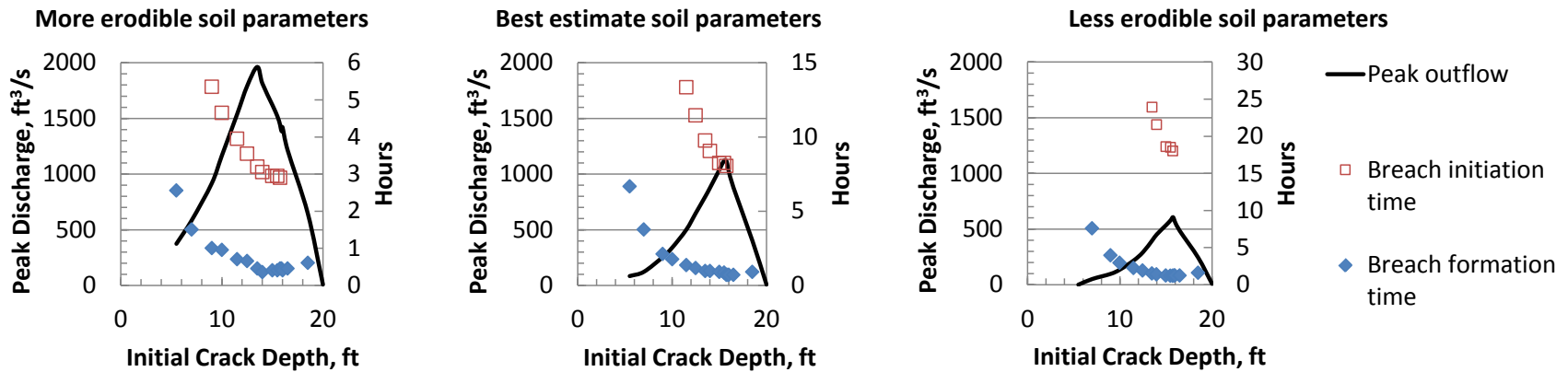


Figure 9. — Breach time and peak breach outflow variation as a function of initial crack depth and soil erodibility parameters. Breach initiation time is the time needed for the headcut to advance into the reservoir following crack formation. Breach formation time is the time from first advance into the reservoir to the time of peak outflow.

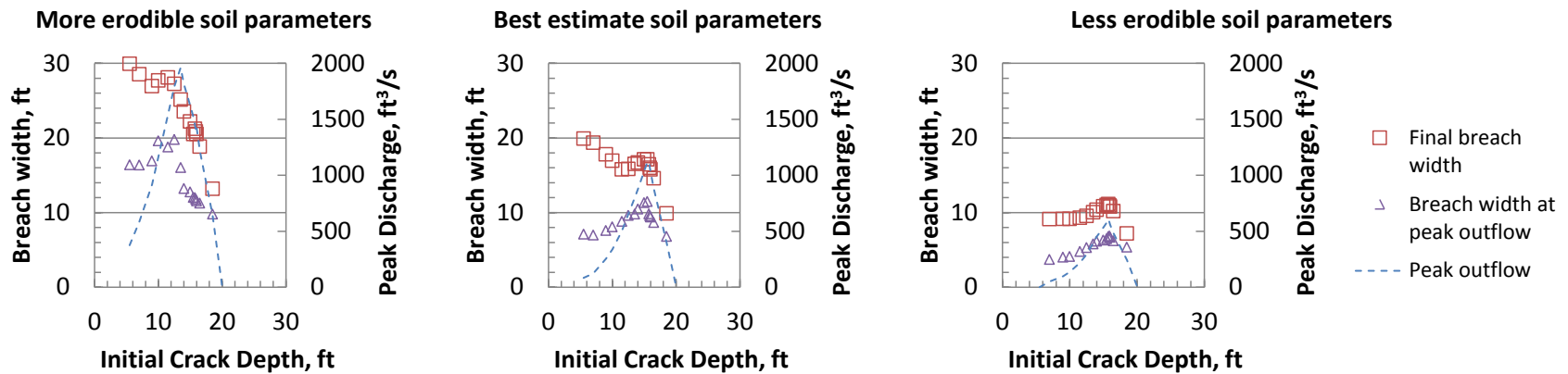


Figure 10. — Breach width variation as a function of initial crack depth and soil erodibility parameters.

Table 6 shows parameter estimates generated by each of these methods, with notes about assumptions made to apply each equation or method. For most of the estimates, a predicted value and range are provided, based on upper and lower bound factors developed by Wahl (2004). Except for the Walder & O'Connor method, none of these prediction methods consider the erodibility of the embankment materials.

The regression-based estimates of breach formation time compare reasonably well to the WinDAM B results, with the regression-based best-estimate values falling within or close to the range of the more erodible and less erodible scenarios modeled in WinDAM B. The regression-based estimates of breach width and peak breach outflow do not compare as well. All of the breach width and peak outflow estimates are outside of the range of the WinDAM B results, some very significantly. The results differ so significantly because the regression-based methods do not consider the effects of soil erodibility, and because the reservoir in this case is relatively small and drains before the breach width can increase to sizes comparable to those predicted by the regression equations. The database of dam failures used to develop most of the regression equations probably includes a significant percentage of dams that impounded relatively large reservoirs and were constructed with highly erodible soils. Terminal Dam is believed to be less erodible than most of the embankments used to develop the regression equations.

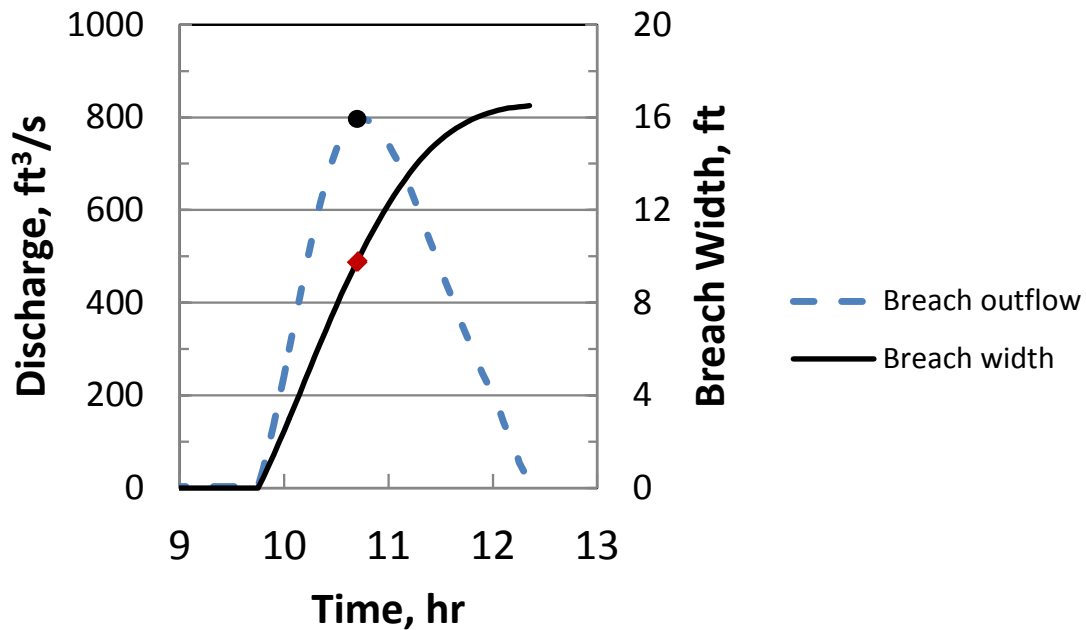


Figure 11. — Typical evolution of breach outflow and breach width. Breach width at the time of peak outflow is about 50 to 65% of the final breach width achieved as the reservoir drains.

Table 6. — Breach parameter predictions using regression equations, and comparison to WinDAM B modeling results. For regression equations, the best-estimate predicted value is shown first, with upper and lower bounds in parentheses [based on analysis by Wahl (2004)].

Method	Breach width, ft	Breach formation time, hr	Peak breach outflow, ft ³ /s
Von Thun & Gillette (1990) *	69 (26-125)	0.88 (0.31-15)	
Froehlich (1995a)	39 (16-93)	0.23 (0.09-1.7)	
Froehlich (1995b)			6,600 (3,500-15,200)
Walder & O'Connor (1997) **			3,900 (600-14,100)
Froehlich (2008)	56	0.29	
WinDAM B	11.5 (7-20) <i>(at time of peak outflow)</i>	0.7 (0.35-1.2)	1,120 (605-1960)
	17.1 (11-30) <i>(final)</i>		

* Time parameter for Von Thun & Gillette (1990) is estimated using their equation based on average predicted breach width and height of dam. (Other equations were also given by Von Thun & Gillette.)

** Assumes embankment is erosion resistant, based on clay content, PI, and jet test results.

Effect of Embankment Modification

A proposed modification to address seismic issues is to thicken the crest of both embankments to 50 ft and maintain the downstream slope at 2H:1V. This increases the distance that a headcut must advance to breach into the reservoir by 30 ft. A series of WinDAM B simulations was carried out using the best estimate soil parameters to determine the change in breach behavior caused by this modification. The resulting breach outflow hydrograph was almost identical to that obtained for the existing embankment, except that the time needed for breach initiation was extended about 27% from 8.25 to 10.5 hr. The breach formation time remained the same at about 0.7 to 0.75 hr, and the peak breach outflow was almost identical to that obtained with the existing embankment section.

These results may seem surprising at first, but they are consistent with the erosion process models in WinDAM B. Because flow through the crack is modeled as a weir flow, thickening the embankment and lengthening the flow path causes no significant change in the initial discharge through the crack. The rate of headcut advance remains the same because the unit discharge and head drop are unchanged, but the headcut must advance 30 ft further to initiate a breach. In the time required for the additional headcut advance, the reservoir drains further (at a slow rate through the crack), so slightly less head is available during the breach formation and widening phases. However, the breach widening rate remains about the same also, because the widening rate is a function of the applied shear stress and the soil erosion resistance, and the shear stress is considered to be only a function of the reservoir head and the resulting critical depth of flow through the breach opening. WinDAM B does not give consideration to the effect of a longer flow path through the embankment (which might reduce the shear stress), nor does it consider whether the rate of erosion needed to achieve a certain widening rate might exceed the sediment transport capacity of the flow. WinDAM B always assumes that erosion is a detachment rate-limited process and that the flow through the breach will have sufficient

transport capacity to remove soil more rapidly than it can be detached. Ultimately, the peak breach outflow for the modified embankment is reduced by less than 1% from the value predicted for the existing embankment. A similar result would be expected if the modified embankment were modeled using the more erodible and less erodible sets of soil properties.

Summary and Conclusions

Submerged jet erosion tests conducted on the embankments at Terminal Dam provided quantitative estimates of the critical shear stress and detachment rate coefficients for the embankments that were consistent with the known soil properties. These erodibility parameters and undrained shear strength values estimated from previous field and laboratory measurements were used as inputs to the WinDAM B dam breach model. The model was used to simulate dam breaches triggered by the development of a transverse crack through the dam during a seismic event. Cracks of varying depth were modeled, and the peak breach outflows occurred with crack depths between 13.5 and 15.75 ft, depending on the specific values of the soil erodibility parameters.

For the best estimate soil erodibility parameters, WinDAM B predicted a breach initiation time of 8 hours, a breach formation time of 0.7 hr, a peak outflow of 1120 ft³/s, and an average breach width at the time of peak outflow equal to 11.5 ft. Assuming a more erodible set of soil parameters reduced the breach initiation time to 3 hr, breach formation time was reduced to 0.35 hr, peak outflow increased to 1960 ft³/s, and breach width increased to 20 ft. With a less erodible set of soil parameters, the breach initiation time increased to 18 hr, breach formation time increased to 1.2 hr, peak outflow dropped to 605 ft³/s, and breach width was only 7 ft. A series of simulations performed with a modified (thickened) embankment section and best estimate soil parameters showed that the only significant effect on breach behavior of the modified section was to increase the breach initiation time by about 25%. To support inundation analyses being performed for the downstream area, Appendix B contains detailed breach hydrographs for the crack depths producing maximum peak breach outflows for each combination of embankment geometry and soil parameters.

A comparison to regression equations commonly used for breach parameter and peak breach outflow prediction showed that the regression equations predicted similar breach times but wider breach widths and larger peak outflows. The spread between lower and upper bound predictions with the regression equations was also much greater than the variation seen in the WinDAM B results using the more and less erodible soil parameter inputs. The ability to measure erodibility parameters and apply a model that simulates the real effects of changes in erodibility produces less severe estimates of dam breach flooding conditions and increased confidence in results, as indicated by the narrower range of lower and upper bound estimates. The significant reductions in breach width and peak outflow are primarily due to the erosion resistance of the embankment soils and the small size of the reservoir.

Cited References

- [1] ASTM, 2007. Standard D-5852. Standard test method for erodibility determination of soil in the field or in the laboratory by the jet index method. *Annual Book of ASTM Standards*, Section 4: Construction, Vol. 04.08. Philadelphia, Penn.: American Society for Testing and Materials.
- [2] Froehlich, D.C., 1995a, “Embankment Dam Breach Parameters Revisited,” *Water Resources Engineering*, Proceedings of the 1995 ASCE Conference on Water Resources Engineering, San Antonio, Texas, August 14-18, 1995, p. 887-891.
- [3] Froehlich, D.C., 1995b, “Peak Outflow from Breached Embankment Dam,” *Journal of Water Resources Planning and Management*, 121(1):90-97.
- [4] Froehlich, D.C., 2008. Embankment dam breach parameters and their uncertainties. *Journal of Hydraulic Engineering*, 134(12):1708-1721.
- [5] Hanson, G.J. and A. Simon. 2001. Erodibility of cohesive streambeds in the loess area of the midwestern USA. *Hydrological Processes*, 15:23-38.
- [6] Hanson, G.J., and K.R. Cook, 2004. Apparatus, test procedures, and analytical methods to measure soil erodibility in situ. *Applied Engineering in Agriculture*, Vol. 20, No. 4, pp. 455-462.
- [7] Hanson, G.J., T.L. Wahl, D.M. Temple, S.L. Hunt, and R.D. Tejral, 2010. Erodibility characteristics of embankment materials. In: *Dam Safety 2010* . Proceedings of the Association of State Dam Safety Officials Annual Conference, September 19-23, 2010, Seattle, WA. (CDROM).
- [8] Hobbs, L., 2004. “Draft Interim Summary Drilling and Hole Completion Report,” Mid Pacific Regional Office, Bureau of Reclamation, Sacramento, California, 2004.
- [9] Schenk McFarland, T., 2010. Technical Memorandum VZ-8313-4, “Terminal Dam Issue Evaluation Risk Analysis”, Bureau of Reclamation, Technical Service Center, Geotechnical Engineering Group 3 (86-68313), December 2010.
- [10] Strauss, T., 2004. “Laboratory Soils Test Results – Terminal Dam, Solano Project, California,” *Memorandum from Thomas Strauss*, Earth Sciences and Research Laboratory Services Group, Bureau of Reclamation, Denver, Colorado, to Mark Pabst, Geotechnical Engineering Group 3, Bureau of Reclamation, Technical Service Center, Denver, Colorado, September 30, 2004. Earth Sciences and Research Laboratory Referral Number 8340-04-16.
- [11] Von Thun, J.L., and D.R. Gillette, 1990, *Guidance on Breach Parameters*, unpublished internal document, U.S. Bureau of Reclamation, Denver, Colorado, March 13, 1990, 17 p.

- [12] Wahl, T.L., P.-L. Regazzoni, and Z. Erdogan, 2008. *Determining Erosion Indices of Cohesive Soils with the Hole Erosion Test and Jet Erosion Test*, Dam Safety Technology Development Report DSO-08-05, U.S. Dept. of the Interior, Bureau of Reclamation, Denver, Colorado, 45 pp.
- [13] Wahl, T.L., 2004. Uncertainty of predictions of embankment dam breach parameters". *Journal of Hydraulic Engineering*, 130(5):389-397.
- [14] Walder, J.S., and J.E. O'Connor, 1997. Methods for predicting peak discharge of floods caused by failure of natural and constructed earth dams. *Water Resources Research*, 33(10): 2337-2348.

Appendix A: WinDAM B Technical References

Hanson, G. J., K. M. Robinson, and K. R. Cook. 2001. Prediction of headcut migration using a deterministic approach. *Transactions of the ASAE*, 44(3):525-531.

Hanson, G.J., and S.L. Hunt, 2007. Lessons learned using laboratory jet method to measure soil erodibility of compacted soils. *Applied Engineering in Agriculture*, 23(3):305-312.

Hanson, G.J., D.M. Temple, S.L. Hunt, and R.D. Tejral, 2011. Development and characterization of soil material parameters for embankment breach. *Applied Engineering in Agriculture*, 27(4):587-595.

Hunt, S.L., G.J. Hanson, K.R. Cook, and K.C. Kadavy, 2005. Breach widening observations from earthen embankment tests. *Transactions of the ASAE*, 48(3):1115-1120.

Temple, D.M., G.J. Hanson, and M.L. Neilsen, 2006. WINDAM – Analysis of overtopped earth embankment dams. ASABE Annual International Meeting, Portland, OR, July 9 – 12, 2006.

Temple, D.M., and W. Irwin, 2006. Allowable overtopping of earthen dams. In: *Dam Safety 2006*. Proceedings of the Association of State Dam Safety Officials Annual Conference, September 10-14, 2006, Boston, Massachusetts. CDROM.

Temple, D.M., G.J. Hanson, and S.L. Hunt, 2010. Observations on dam overtopping breach processes and prediction. *The Journal of Dam Safety*, 8(2):28-33.

Visser, K., G. Hanson, D. Temple, and M. Neilsen, 2012. Earthen embankment overtopping analysis using the WinDAM B software. In: *Dam Safety 2012*. Proceedings of the Association of State Dam Safety Officials Annual Conference, Sept. 16-20, 2012, Denver, CO.

Appendix B: Breach Outflow Hydrographs

Embankment geometry	Existing			Modified
Soil parameters	Best estimate	Less erodible	More erodible	Best estimate
Initial crack depth, ft	15.5	15.75	13.5	15.75
Time, hr	Overtop Q / Breach Q (ft ³ /s)			
0.05	4.73	4.89	3.55	4.84
0.1	4.73	4.89	3.55	4.84
0.15	4.73	4.89	3.55	4.84
0.2	4.73	4.88	3.55	4.84
0.25	4.73	4.88	3.55	4.84
0.3	4.73	4.88	3.55	4.84
0.35	4.73	4.88	3.55	4.84
0.4	4.72	4.88	3.55	4.83
0.45	4.72	4.88	3.55	4.83
0.5	4.72	4.88	3.54	4.83
0.55	4.72	4.88	3.54	4.83
0.6	4.72	4.88	3.54	4.83
0.65	4.72	4.87	3.54	4.83
0.7	4.72	4.87	3.54	4.83
0.75	4.72	4.87	3.54	4.83
0.8	4.72	4.87	3.54	4.83
0.85	4.71	4.87	3.54	4.82
0.9	4.71	4.87	3.54	4.82
0.95	4.71	4.87	3.54	4.82
1	4.71	4.87	3.54	4.82
1.05	4.71	4.87	3.54	4.82
1.1	4.71	4.86	3.54	4.82
1.15	4.71	4.86	3.54	4.82
1.2	4.71	4.86	3.53	4.82
1.25	4.71	4.86	3.53	4.82
1.3	4.70	4.86	3.53	4.81
1.35	4.70	4.86	3.53	4.81
1.4	4.70	4.86	3.53	4.81
1.45	4.70	4.86	3.53	4.81
1.5	4.70	4.86	3.53	4.81
1.55	4.70	4.85	3.53	4.81
1.6	4.70	4.85	3.53	4.81

Embankment geometry	Existing			Modified
Soil parameters	Best estimate	Less erodible	More erodible	Best estimate
Initial crack depth, ft	15.5	15.75	13.5	15.75
Time, hr	Overtop Q / Breach Q (ft ³ /s)			
1.65	4.70	4.85	3.53	4.81
1.7	4.70	4.85	3.53	4.81
1.75	4.70	4.85	3.53	4.81
1.8	4.69	4.85	3.53	4.80
1.85	4.69	4.85	3.52	4.80
1.9	4.69	4.85	3.52	4.80
1.95	4.69	4.84	3.52	4.80
2	4.69	4.84	3.52	4.80
2.05	4.69	4.84	3.52	4.80
2.1	4.69	4.84	3.52	4.80
2.15	4.69	4.84	3.52	4.80
2.2	4.69	4.84	3.52	4.80
2.25	4.68	4.84	3.52	4.79
2.3	4.68	4.84	3.52	4.79
2.35	4.68	4.84	3.52	4.79
2.4	4.68	4.83	3.52	4.79
2.45	4.68	4.83	3.52	4.79
2.5	4.68	4.83	3.52	4.79
2.55	4.68	4.83	3.51	4.79
2.6	4.68	4.83	3.51	4.79
2.65	4.68	4.83	3.51	4.79
2.7	4.68	4.83	3.51	4.78
2.75	4.67	4.83	3.51	4.78
2.8	4.67	4.83	3.51	4.78
2.85	4.67	4.83	3.51	4.78
2.9	4.67	4.82	3.51	4.78
2.95	4.67	4.82	3.51	4.78
3	4.67	4.82	3.51	4.78
3.05	4.67	4.82	3.51	4.78
3.1	4.67	4.82	3.51	4.78
3.15	4.67	4.82	3.51	4.77
3.2	4.66	4.82	3.51	4.77
3.25	4.66	4.82	160.53	4.77
3.3	4.66	4.82	354.48	4.77
3.35	4.66	4.81	572.53	4.77

Embankment geometry	Existing			Modified
Soil parameters	Best estimate	Less erodible	More erodible	Best estimate
Initial crack depth, ft	15.5	15.75	13.5	15.75
Time, hr	Overtop Q / Breach Q (ft ³ /s)			
3.4	4.66	4.81	801.31	4.77
3.45	4.66	4.81	1045.31	4.77
3.5	4.66	4.81	1295.76	4.77
3.55	4.66	4.81	1542.29	4.77
3.6	4.66	4.81	1770.84	4.76
3.65	4.66	4.81	1961.62	4.76
3.7	4.65	4.81	1857.25	4.76
3.75	4.65	4.81	1761.39	4.76
3.8	4.65	4.80	1735.28	4.76
3.85	4.65	4.80	1606.92	4.76
3.9	4.65	4.80	1469.22	4.76
3.95	4.65	4.80	1408.13	4.76
4	4.65	4.80	1263.15	4.76
4.05	4.65	4.80	1169.56	4.75
4.1	4.65	4.80	1010.51	4.75
4.15	4.64	4.80	885.24	4.75
4.2	4.64	4.80	633.34	4.75
4.25	4.64	4.79		4.75
4.3	4.64	4.79		4.75
4.35	4.64	4.79		4.75
4.4	4.64	4.79		4.75
4.45	4.64	4.79		4.75
4.5	4.64	4.79		4.75
4.55	4.64	4.79		4.74
4.6	4.64	4.79		4.74
4.65	4.63	4.79		4.74
4.7	4.63	4.78		4.74
4.75	4.63	4.78		4.74
4.8	4.63	4.78		4.74
4.85	4.63	4.78		4.74
4.9	4.63	4.78		4.74
4.95	4.63	4.78		4.74
5	4.63	4.78		4.73
5.05	4.63	4.78		4.73
5.1	4.62	4.78		4.73

Embankment geometry	Existing			Modified
Soil parameters	Best estimate	Less erodible	More erodible	Best estimate
Initial crack depth, ft	15.5	15.75	13.5	15.75
Time, hr	Overtop Q / Breach Q (ft ³ /s)			
5.15	4.62	4.77		4.73
5.2	4.62	4.77		4.73
5.25	4.62	4.77		4.73
5.3	4.62	4.77		4.73
5.35	4.62	4.77		4.73
5.4	4.62	4.77		4.73
5.45	4.62	4.77		4.72
5.5	4.62	4.77		4.72
5.55	4.62	4.77		4.72
5.6	4.61	4.76		4.72
5.65	4.61	4.76		4.72
5.7	4.61	4.76		4.72
5.75	4.61	4.76		4.72
5.8	4.61	4.76		4.72
5.85	4.61	4.76		4.72
5.9	4.61	4.76		4.72
5.95	4.61	4.76		4.71
6	4.61	4.76		4.71
6.05	4.61	4.76		4.71
6.1	4.60	4.75		4.71
6.15	4.60	4.75		4.71
6.2	4.60	4.75		4.71
6.25	4.60	4.75		4.71
6.3	4.60	4.75		4.71
6.35	4.60	4.75		4.71
6.4	4.60	4.75		4.70
6.45	4.60	4.75		4.70
6.5	4.60	4.75		4.70
6.55	4.60	4.74		4.70
6.6	4.59	4.74		4.70
6.65	4.59	4.74		4.70
6.7	4.59	4.74		4.70
6.75	4.59	4.74		4.70
6.8	4.59	4.74		4.70
6.85	4.59	4.74		4.69

Embankment geometry	Existing			Modified
Soil parameters	Best estimate	Less erodible	More erodible	Best estimate
Initial crack depth, ft	15.5	15.75	13.5	15.75
Time, hr	Overtop Q / Breach Q (ft ³ /s)			
6.9	4.59	4.74		4.69
6.95	4.59	4.74		4.69
7	4.59	4.73		4.69
7.05	4.58	4.73		4.69
7.1	4.58	4.73		4.69
7.15	4.58	4.73		4.69
7.2	4.58	4.73		4.69
7.25	4.58	4.73		4.69
7.3	4.58	4.73		4.69
7.35	4.58	4.73		4.68
7.4	4.58	4.73		4.68
7.45	4.58	4.72		4.68
7.5	4.58	4.72		4.68
7.55	4.57	4.72		4.68
7.6	4.57	4.72		4.68
7.65	4.57	4.72		4.68
7.7	4.57	4.72		4.68
7.75	4.57	4.72		4.68
7.8	4.57	4.72		4.67
7.85	4.57	4.72		4.67
7.9	4.57	4.72		4.67
7.95	4.57	4.71		4.67
8	4.57	4.71		4.67
8.05	4.56	4.71		4.67
8.1	4.56	4.71		4.67
8.15	4.56	4.71		4.67
8.2	4.56	4.71		4.67
8.25	4.56	4.71		4.67
8.3	76.33	4.71		4.66
8.35	158.59	4.71		4.66
8.4	246.04	4.70		4.66
8.45	337.70	4.70		4.66
8.5	432.44	4.70		4.66
8.55	526.90	4.70		4.66
8.6	619.83	4.70		4.66

Embankment geometry	Existing			Modified
Soil parameters	Best estimate	Less erodible	More erodible	Best estimate
Initial crack depth, ft	15.5	15.75	13.5	15.75
Time, hr	Overtop Q / Breach Q (ft ³ /s)			
8.65	709.60	4.70		4.66
8.7	794.53	4.70		4.66
8.75	873.09	4.70		4.65
8.8	943.98	4.70		4.65
8.85	1004.53	4.70		4.65
8.9	1053.78	4.69		4.65
8.95	1088.81	4.69		4.65
9	1107.58	4.69		4.65
9.05	1118.96	4.69		4.65
9.1	1120.97	4.69		4.65
9.15	1102.74	4.69		4.65
9.2	1075.94	4.69		4.65
9.25	1048.81	4.69		4.64
9.3	1013.12	4.69		4.64
9.35	967.39	4.68		4.64
9.4	920.57	4.68		4.64
9.45	873.54	4.68		4.64
9.5	821.42	4.68		4.64
9.55	768.94	4.68		4.64
9.6	707.97	4.68		4.64
9.65	649.14	4.68		4.64
9.7	579.09	4.68		4.63
9.75	510.92	4.68		4.63
9.8	374.79	4.68		4.63
9.85		4.67		4.63
9.9		4.67		4.63
9.95		4.67		4.63
10		4.67		4.63
10.05		4.67		4.63
10.1		4.67		4.63
10.15		4.67		4.63
10.2		4.67		4.62
10.25		4.67		4.62
10.3		4.66		4.62
10.35		4.66		4.62

Embankment geometry	Existing			Modified
Soil parameters	Best estimate	Less erodible	More erodible	Best estimate
Initial crack depth, ft	15.5	15.75	13.5	15.75
Time, hr	Overtop Q / Breach Q (ft ³ /s)			
10.4		4.66		4.62
10.45		4.66		4.62
10.5		4.66		4.62
10.55		4.66		79.34
10.6		4.66		164.89
10.65		4.66		255.84
10.7		4.66		351.16
10.75		4.66		448.72
10.8		4.65		546.11
10.85		4.65		641.85
10.9		4.65		734.08
10.95		4.65		821.06
11		4.65		901.18
11.05		4.65		973.10
11.1		4.65		1032.77
11.15		4.65		1081.71
11.2		4.65		1107.90
11.25		4.64		1117.45
11.3		4.64		1117.52
11.35		4.64		1102.17
11.4		4.64		1071.04
11.45		4.64		1041.32
11.5		4.64		1011.02
11.55		4.64		970.21
11.6		4.64		926.58
11.65		4.64		882.40
11.7		4.64		838.80
11.75		4.63		788.64
11.8		4.63		740.13
11.85		4.63		682.01
11.9		4.63		625.84
11.95		4.63		559.55
12		4.63		480.68
12.05		4.63		330.76

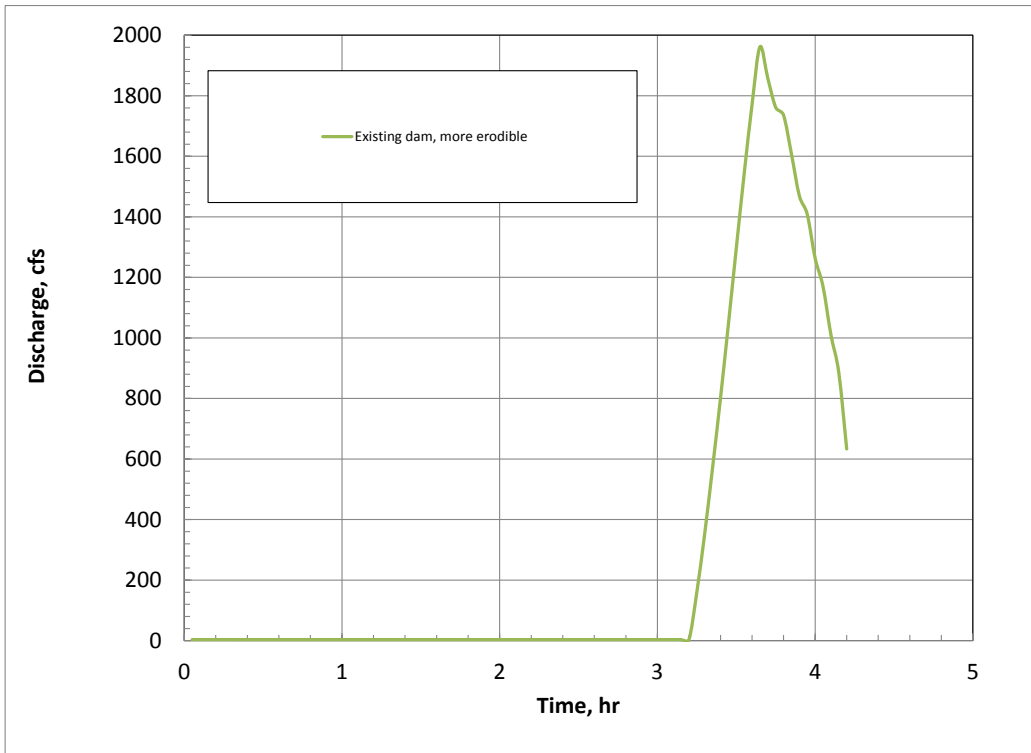


Figure B1. — Breach outflow hydrograph for existing dam configuration assuming more erodible soil parameters and worst-case initial crack depth.

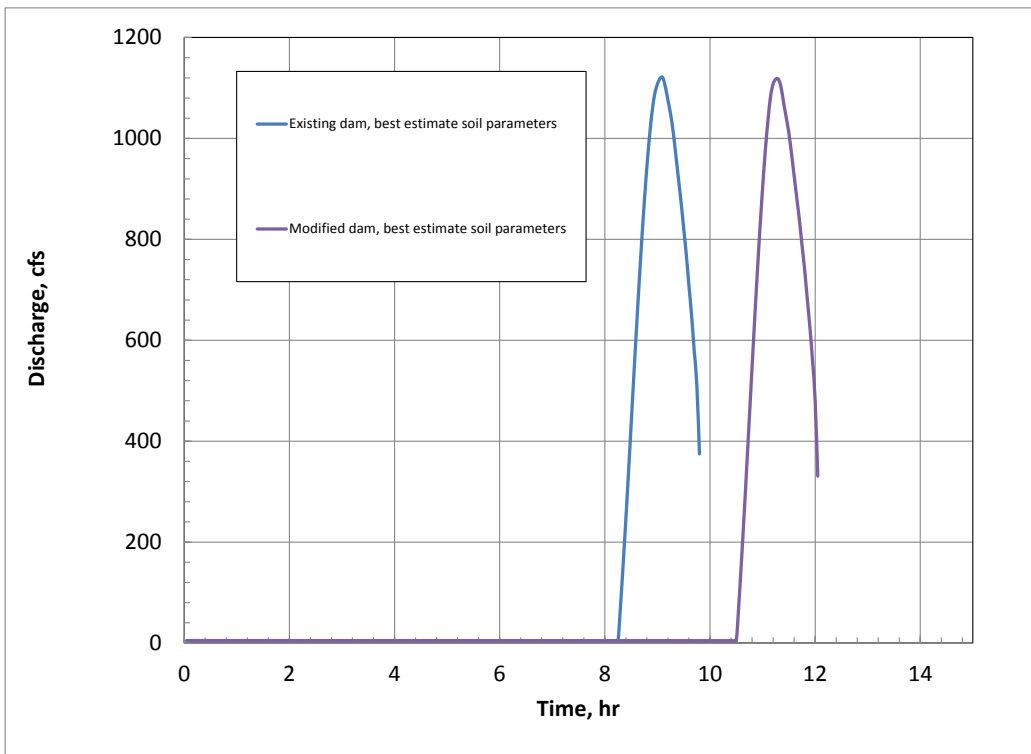


Figure B2. — Breach outflow hydrographs for existing dam and modified dam assuming best-estimate soil parameters and worst-case initial crack depth.

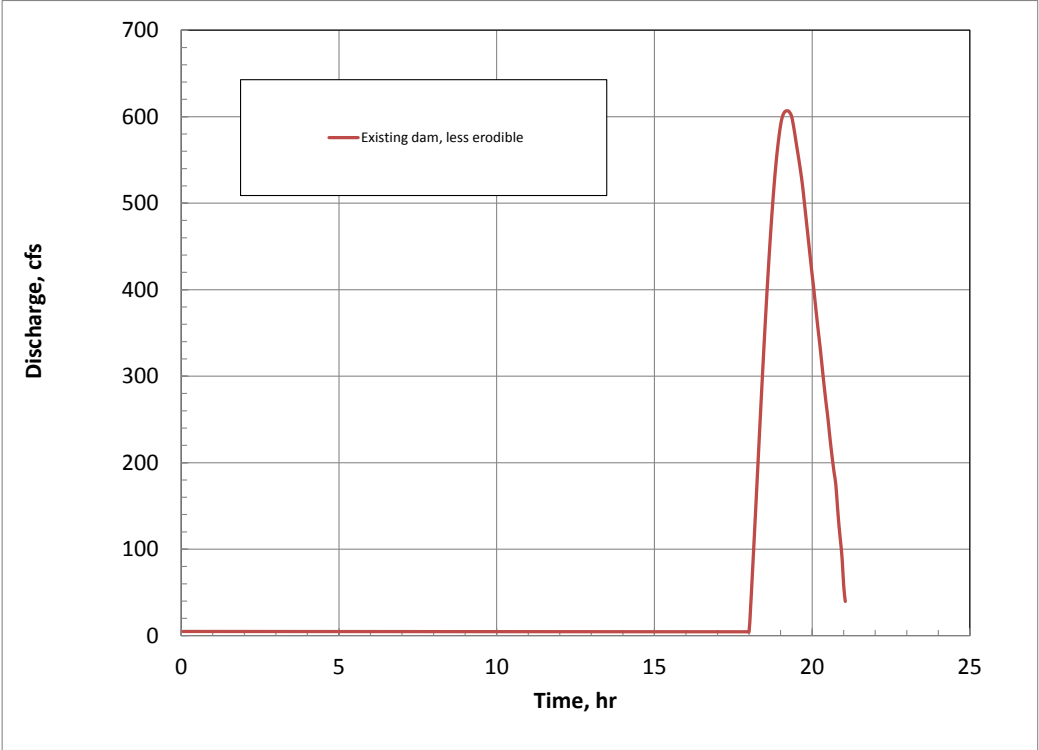


Figure B2. — Breach outflow hydrograph for existing dam assuming less erodible soil parameters and worst-case initial crack depth.

Appendix C: WinDAM B Simulations to Test Effect of Initial Crack Width

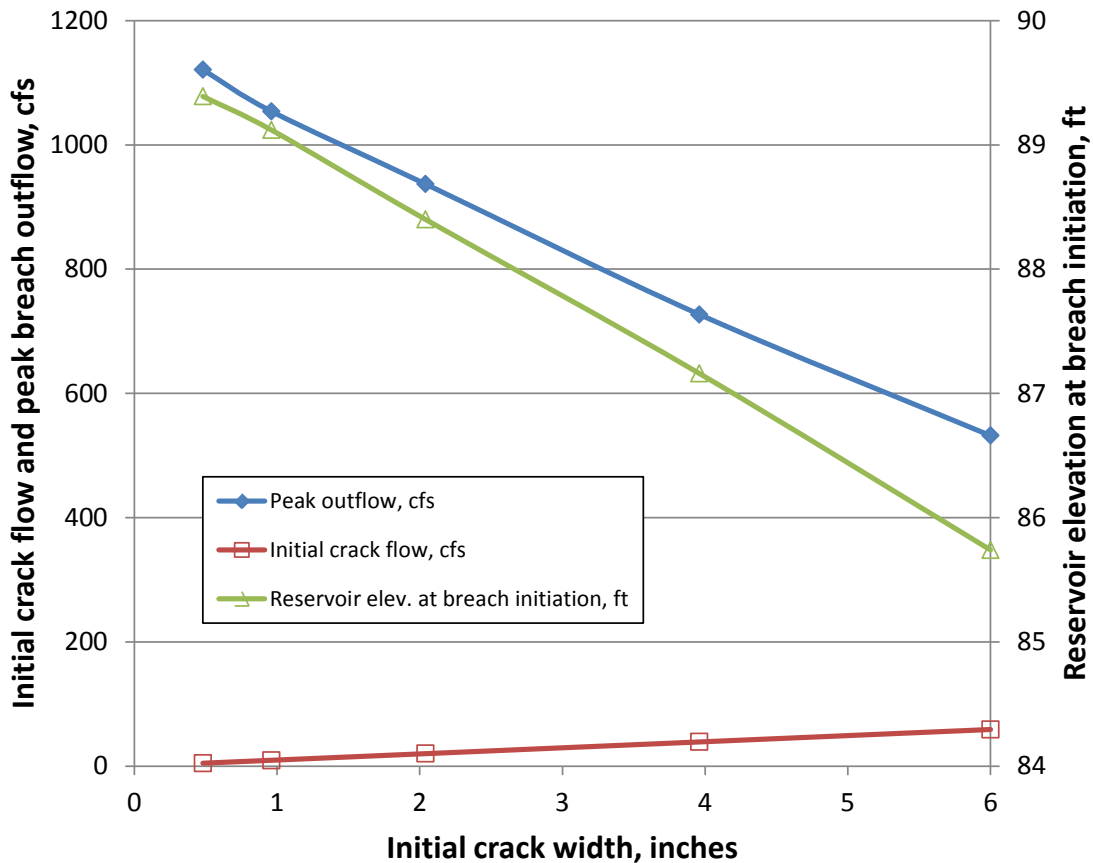


Figure C1. — Results of simulations carried out over a range of initial crack widths, using best-estimate soil parameters and a crack depth of 15.5 ft (which produced maximum peak outflow for the ½-inch wide crack). A wider initial crack allows greater outflow and more reservoir drawdown during the breach initiation phase. The headcut advance rate for all cases is similar because it depends on unit discharge through the crack, not total discharge. The end result is a significant reduction of peak breach outflow as the initial crack width is increased.